Published for SISSA by Springer

Received: November 9, 2014
Revised: January 3, 2015
Accepted: January 18, 2015
Published: February 11, 2015

Reduced modified Chaplygin gas cosmology

Jianbo Lu,[a] Danhua Geng,[a] Lixin Xu,[b] Yabo Wu[a] and Molin Liu[c]

[a] *Department of Physics, Liaoning Normal University, Dalian 116029, P. R. China*

[b] *School of Physics and Optoelectronic Technology, Dalian University of Technology, Dalian, 116024, P. R. China*

[c] *College of Physics and Electronic Engineering, Xinyang Normal University, Xinyang 464000, P.R. China*

E-mail: lvjianbo819@163.com, danhuageng@163.com, lxxu@dlut.edu.cn, ybwu1961@163.com, mlliu@163.com

Abstract: In this paper, we study cosmologies containing the reduced modified Chaplygin gas (RMCG) fluid which is reduced from the modified Chaplygin gas $p = A\rho - B\rho^{-\alpha}$ for the value of $\alpha = -1/2$. In this special case, dark cosmological models can be realized for different values of model parameter A. We investigate the viabilities of these dark cosmological models by discussing the evolutions of cosmological quantities and using the currently available cosmic observations. It is shown that the special RMCG model ($A = 0$ or $A = 1$) which unifies the dark matter and dark energy should be abandoned. For $A = 1/3$, RMCG which unifies the dark energy and dark radiation is the favorite model according to the objective Akaike information criteria. In the case of $A < 0$, RMCG can achieve the features of the dynamical quintessence and phantom models, where the evolution of the universe is not sensitive to the variation of model parameters.

Keywords: Cosmology of Theories beyond the SM, Classical Theories of Gravity

ArXiv ePrint: 1312.0779

doi:10.1007/JHEP02(2015)071

JHEP02(2015)071

Contents

1 Introduction

Observations indicate some challenges to the standard Big Bang model of cosmology. Several invisible components what we have to search in universe are hinted. For example, the observations on rotation curve of galaxy [1] directly relate to the amount of pressureless matter, proposing dark matter (DM) in our Universe; the observations on supernovae of type Ia [2, 3] point out an accelerating universe at late time, which is usually interpreted as the existence of a new ingredient called dark energy (DE); the Wilkinson microwave anisotropy probe (WMAP) provides precise measurement of the cosmic microwave background radiation. Combining the 9-year WMAP results with the Hubble constant measured from the Hubble Space Telescope (HST) and the baryons acoustic oscillations (BAO) from the SDSS puts a constraint on the effective number of relativistic degrees of freedom $N_{\rm eff} = 3.84 \pm 0.4$ which implies the presence of an extra dark radiation (DR) component at 95% confidence level [4, 5].[1] It is interesting to search origins of these dark sectors. In the past years, efforts were made to study these dark sectors comprising the DM, DE

[1] Recently, ref. [6] studied the effect of H_0 prior on the value of $N_{\rm eff}$. In the ΛCDM model, the evidence of DR is weakened to ~ 1.2 standard deviations ($N_{\rm eff} = 3.52 \pm 0.39$ at 68% confidence level) [6] by taking the median statistics (MS) prior $H_0 = 68 \pm 2.8$ km s^{-1}Mpc^{-1} to replace the HST prior $H_0 = 73.8 \pm 2.4$ km s^{-1}Mpc^{-1}. This result tends to show that the evidence for DR is not pressing any more.

and DR, such as the seeking for the candidates of the cold and warm dark matter [7, 8], the discussion on the cosmological constant and the dynamical DE [9–21], the exploration for the origins of DR using the decayed particle [22, 23], the interacting DM [24], the Horava-Lifshitz gravity [25, 26] and extra dimensions [27], etc.

In addition to these dark sectors (DM, DE, DR), baryon and radiation as visible constituents naturally exist in our Universe. Current cosmic observations suggest that our Universe contains about 70% the negative-pressure DE, 30% the pressureless matter (or called dust) including the DM and baryon, and a small fraction of radiation components which are composed of the photon, neutrino as well as additional relativistic species [28]. Someone proposed an economical model which can unify the DM and DE in a single fluid, say the generalized Chaplygin gas [29–32] and the modified Chaplygin gas (MCG) [33, 34] for instances. In this paper we will perform new search of dark sectors from the reduced MCG (RMCG) fluid. We study the RMCG fluid using the analyses of theoretical constraints and the comparisons with the observational data, and obtain several interesting properties such as the DE and DR can be uniformly described by this single fluid, the evolutions of the cosmological quantities in the dynamical RMCG model are not sensitive to the variation of model-parameter values, and so on.

This paper is organized as follows. In the next section, we introduce the dark models in the RMCG cosmology. In section III, we examine the evolutions of growth factor and Hubble parameter in the RMCG model, and compare them with the current observational data. The parameter evaluation and model comparison for the RMCG model are performed in section IV. section V is the conclusions.

2 Dark models in RMCG cosmology

The MCG model was widely studied for explaining the cosmic inflation [35–38] or providing an unified model of the DM and DE [39–42]. We consider the equation of state (EoS)

$$p = A\rho - B\rho^{1/2}, \tag{2.1}$$

dubbed as the RMCG, which is reduced from the modified Chaplygin gas $p = A\rho - B\rho^{-\alpha}$ for the constant model parameter $\alpha = -1/2$. This model (2.1) can produce a emergent universe without the time singularity [43–46]. But in this paper, we will take this RMCG fluid as the dark components in our Universe.

Using the energy conservation equation $d\rho/dt = -3H(\rho + p)$, we obtain the energy density of the RMCG fluid,

$$\begin{aligned}
\rho_{RMCG}(a) &= \left[\frac{B}{(1+A)} + \frac{C}{1+A}a^{\frac{-3(1+A)}{2}}\right]^2 \\
&= \rho_{0RMCG}\left[A_s^2 + (1-A_s)^2 a^{-3(1+A)} + 2A_s(1-A_s)a^{\frac{-3(1+A)}{2}}\right] \\
&= \rho_1 + \rho_2 a^{-3(1+A)} + \rho_3 a^{\frac{-3(1+A)}{2}},
\end{aligned} \tag{2.2}$$

where C is an integration constant, $A_s = B\rho_{0RMCG}^{-1/2}/(1+A)$. ρ_1, ρ_2 and ρ_3 are current values of three energy densities in the RMCG fluid. According to eq. (2.2), some unified

JHEP02(2015)071

	$A=1$	$A=\frac{1}{3}$	$A=0$	$-1<A<0$	$A<-1$
$-1<w_0<-\frac{1}{3}$	$1>A_s>\frac{2}{3}$	$1>A_s>\frac{1}{2}$	$1>A_s>\frac{1}{3}$	$1>A_s>\frac{1+3A}{3(1+A)}$	$\frac{1+3A}{3(1+A)}>A_s>1$
$w_0<-1$	$A_s>1$	$A_s>1$	$A_s>1$	$A_s>1$	$A_s<1$

Table 1. Theoretical constraints on RMCG model parameter A_s by assuming $-1<w_0<-1/3$ (quintessence) and $w_0<-1$ (phantom), where the different values or intervals for parameter A are adopted in prior.

models can be achieved for different values of parameter A. Fixing A to zero, we have a unified model containing the DM, DE and cosmic component having $w=p/\rho=-1/2$. For $A=1$, the RMCG unifies the DE, DM and stiff matter ($w=1$). In the case of $A=1/3$, a unified model including the DE, DR and exotic component ($w=-1/3$) can be arrived. If A is a free positive model parameter ($A\neq 0,1,1/3$), we obtain a unified model comprising the DE and an unknown component. In the range of $A<0$, RMCG fluid plays the role as the phantom-like ($A<-1$) and quintessence-like ($0>A>-1$) dynamical DE. In a spatial flat Friedmann-Robertson-Walker (FRW) universe containing the RMCG fluid, one has the Friedmann equation

$$\begin{aligned} H^2(a)/H_0^2 &= \Omega_{0i}a^{-3(1+w_i)}+\Omega_{RMCG}(a) \\ &= \Omega_{0i}a^{-3(1+w_i)}+(1-\Omega_{0i})\left[A_s^2+(1-A_s)^2a^{-3(1+A)}+2A_s(1-A_s)a^{\frac{-3(1+A)}{2}}\right] \\ &= \Omega_{0i}a^{-3(1+w_i)}+\Omega_{01}+\Omega_{02}a^{-3(1+A)}+\Omega_{03}a^{\frac{-3(1+A)}{2}}, \end{aligned} \tag{2.3}$$

where Ω_{0i} is the current dimensionless energy density beyond the dark sectors, Ω_{01}, Ω_{02} and Ω_{03} correspond to three current dimensionless energy densities given by the RMCG fluid. a is the scale factor that is related to cosmic redshift by $a=1/(1+z)$. In the following, we show expressions of some basic cosmological parameters in the RMCG model:

(1) The adiabatic sound speed for the RMCG fluid, $c_s^2=\delta p/\delta\rho=A-\frac{\frac{1}{2}(1+A)A_s}{A_s+(1-A_s)a^{-\frac{3}{2}(1+A)}}$. A small non-negative sound speed for matter component is necessary for forming the large scale structure of our Universe.

(2) Equation of state for the RMCG fluid, $w=p/\rho=A-\frac{(1+A)A_s}{A_s+(1-A_s)a^{-\frac{3}{2}(1+A)}}$. To obtain a late time accelerating expansion universe, it should be respected that the current value of EoS $w_0<-\frac{1}{3}$. Table 1 lists the theoretical constraints on model parameter A_s in the RMCG cosmology by locating the w_0 at the quintessence region or phantom region, where the different values or intervals for model parameter A are adopted.

(3) Deceleration parameter $q(a)=-\ddot{a}/(aH^2)$. An expanding universe having a transition from deceleration to acceleration is consistent with the current cosmic observations.

(4) Dimensionless density parameter $\Omega_j=\rho_j/\rho_c$. $\rho_c=3H^2/(8\pi G)$ is the critical density, and j denotes the energy component in our Universe.

JHEP02(2015)071

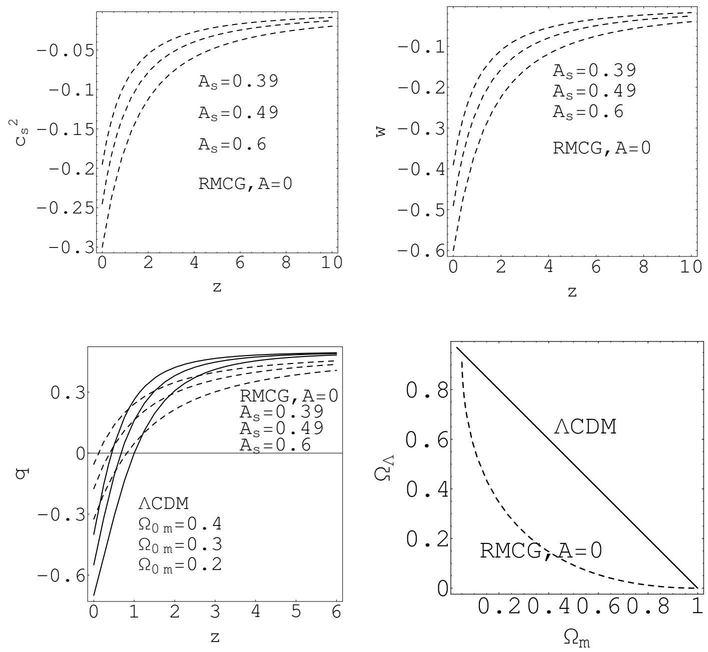

Figure 1. Evolutions of the adiabatic sound speed $c_s^2(z)$, EoS $w(z)$ and deceleration parameter $q(z)$, and values of dimensionless density parameters for the RMCG ($A = 0$) model. Solid lines depict the case of the ΛCDM.

2.1 Should the unified model of DE and DM be ruled out in RMCG cosmology

For $A = 0$ or $A = 1$, a unified model of DE and DM can be obtained. In the case of $A = 0$, the RMCG fluid includes the DM, DE and new hinted dark ingredient ($w = -1/2$), where the Friedmann equation is written as

$$\begin{aligned} H^2(a)/H_0^2 &= \Omega_{0b}a^{-3} + \Omega_{0r}a^{-4} + (1 - \Omega_{0b} - \Omega_{0r})[A_s^2 + (1 - A_s)^2 a^{-3} + 2A_s(1 - A_s)a^{-3/2}] \\ &= \Omega_{0b}a^{-3} + \Omega_{0r}a^{-4} + \Omega_{01} + \Omega_{02}a^{-3} + \Omega_{03}a^{-3/2}, \end{aligned} \tag{2.4}$$

where Ω_{0b} and Ω_{0r} represent the fractional energy densities for baryon and radiation (including all relativistic particles, such as CMB photon $\Omega_{0\gamma}$, neutrino $\Omega_{0\nu}$, etc...), respectively. From eq. (2.4), one easily gets the current dimensionless energy density for the dark energy $\Omega_\Lambda = \Omega_{01} = (1 - \Omega_{0b} - \Omega_{0r})A_s^2$, dark-matter $\Omega_{0dm} = \Omega_{02} = (1 - \Omega_{0b} - \Omega_{0r})(1 - A_s)^2$ and unfound component $\Omega_{0u} = \Omega_{03} = 2(1 - \Omega_{0b} - \Omega_{0r})A_s(1 - A_s)$.

After calculation, one gains $A_s \in (0.39, 0.6)$, $\Omega_\Lambda \in (0.15, 0.34)$ and $\Omega_{0u} \in (0.45, 0.46)$ by setting current values $\Omega_{0r} \sim 0$, $\Omega_{0b} = 0.05$ and $\Omega_{0m} \in (0.2, 0.4)$. It is obvious that the value of DE density is smaller than observations due to the existence of Ω_{0u}. Taking $a = 1$ in eq. (2.4), we have $\sqrt{\Omega_\Lambda} = \sqrt{1 - \Omega_{0b} - \Omega_{0r}} - \sqrt{\Omega_{0dm}}$. Via this relation, the values of Ω_Λ and Ω_{0m} are illustrated in figure 1, where one can read in RMCG model the deviation of density-parameter values from ΛCDM. Furthermore, we can slove $A_s \simeq 0.49$ and $\Omega_\Lambda \simeq 0.23$ when we take $\Omega_{0m} = 0.3$.

Density parameter	Explicit form	Parameter value	EOS
Ω_{0r}	Ω_{0r}	—	$w = 1/3$
Ω_{0b}	Ω_{0b}	0.05	$w = 0$
Ω_{0dm}	$(1-\Omega_{0b}-\Omega_{0r})(1-A_s)^2$	(0.15,0.35)	$w = 0$
Ω_Λ	$(1-\Omega_{0b}-\Omega_{0r})A_s^2$	(0.15,0.34)	$w = -1$
$1-\Omega_\Lambda-\Omega_{0dm}-\Omega_{0b}-\Omega_{0r}$	$(1-\Omega_{0b}-\Omega_{0r})2A_s(1-A_s)$	(0.45,0.46)	$w = -1/2$

Table 2. Values of dimensionless density parameters in RMCG ($A = 0$) cosmology.

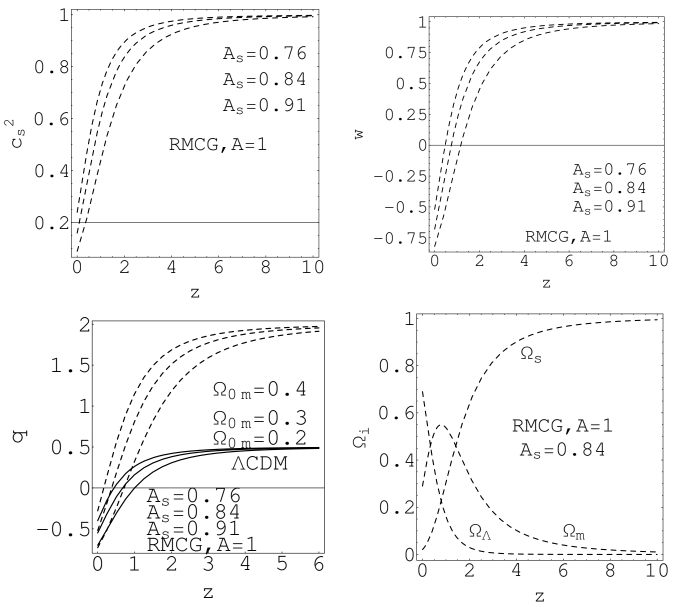

Figure 2. Evolutions of the c_s^2, w, q and Ω_i versus z for the RMCG ($A = 1$) model.

Analyzing the evolution of deceleration parameter $q(z)$, we find in figure 1 that cosmic expansion is translated from deceleration to acceleration, where the current value $q_0 \in (-0.355, -0.056)$ given by the RMCG ($A = 0$) model is larger than $q_0 \in (-0.7, -0.4)$ given by the standard ΛCDM cosmology. For plotting figure 1 we use the parameter values $A_s = [0.39, 0.49, 0.6]$ corresponding to $\Omega_{0m} = [0.2, 0.3, 0.4]$, respectively. From the evolution of $w(z)$ plotted in figure 1, one receives the result that the negative pressure is provided by the RMCG fluid at late time of our Universe. For the evolutions of $c_s^2(z)$, the unexpected negative sound speed is appeared in this RMCG fluid. Since this unified fluid includes dust component, the negative sound speed will induce the classical instability to the system at structure form, where the perturbations on small scales will increase quickly with time and the late time history of the structure formations will be significantly modified [47]. Then it seems that the RMCG (A=0) model is not a good one.

For $A = 1$, RMCG fluid contains the DE, DM and stiff matter ($w = 1$), where the Friedmann equation is expressed by

$$\begin{aligned} H^2(a)/H_0^2 &= \Omega_{0b}a^{-3} + \Omega_{0r}a^{-4} + (1-\Omega_{0b}-\Omega_{0r})[A_s^2 + 2A_s(1-A_s)a^{-3} + (1-A_s)^2a^{-6}] \\ &= \Omega_{0b}a^{-3} + \Omega_{0r}a^{-4} + \Omega_{01} + \Omega_{02}a^{-3} + \Omega_{03}a^{-6}. \end{aligned} \tag{2.5}$$

Density parameter	Explicit form	Parameter value	EOS
Ω_{0r}	Ω_{0r}	—-	$w = 1/3$
Ω_{0b}	Ω_{0b}	0.05	$w = 0$
Ω_{0dm}	$2(1-\Omega_{0b}-\Omega_{0r})A_s(1-A_s)$	(0.15,0.35)	$w = 0$
Ω_Λ	$(1-\Omega_{0b}-\Omega_{0r})A_s^2$	(0.55,0.79)	$w = -1$
$1-\Omega_\Lambda-\Omega_{0dm}-\Omega_{0b}-\Omega_{0r}$	$(1-\Omega_{0b}-\Omega_{0r})(1-A_s)^2$	(0.01,0.05)	$w = 1$

Table 3. Values of dimensionless density parameters in RMCG ($A = 1$) cosmology.

One from eq. (2.5) gains $\Omega_\Lambda = \Omega_{01} = (1-\Omega_{0b}-\Omega_{0r})A_s^2$, $\Omega_{0dm} = \Omega_{02} = 2(1-\Omega_{0b}-\Omega_{0r})A_s(1-A_s)$ and $\Omega_{0s} = \Omega_{03} = (1-\Omega_{0b}-\Omega_{0r})(1-A_s)^2$. Taking $\Omega_{0m} \in (0.2, 0.4)$, we receive $A_s \in (0.76, 0.91)$, $\Omega_\Lambda \in (0.55, 0.79)$ and $\Omega_{0s} \in (0.01, 0.05)$, which are listed in table 3. For this case, $\Omega_{0m} = 0.3$ gives $\Omega_\Lambda = 0.67$.

Figure 2 illustrates the evolutions of the adiabatic sound speed, EoS, deceleration parameter and dimensionless energy density in the RMCG ($A = 1$). As we can see, the value of EoS is transited from the positive to the negative. Correspondingly, a transition from decelerating-expansion universe to accelerating-expansion universe can be realized. Meanwhile, this RMCG unified fluid at hand would not bring the negative value of the adiabatic sound speed. But it has other problems we have to face, such as (1) deceleration parameter is $q > \frac{1}{2}$ at high redshift, which is not satisfied with $q \leq \frac{1}{2}$ in the matter-dominate universe. Matter-dominate universe is necessary for structure formation; (2) Radiation-dominate universe will not appear in this RMCG universe, because of stiff matter. From these points, it seems that this model is not consistent with the current observational universe.

2.2 A unified model of dark energy and dark radiation in RMCG cosmology

Combined analysis of several cosmological data hints the existence of an extra relativistic-energy component (called dark radiation) in the early universe, in addition to the well-known three neutrino species predicted by the standard model of particle physics. The total amount of this extra DR component is often related to the parameter $N_{\rm eff}$ denoting the effective number of relativistic degrees of freedom, which has relation to the energy density of relativistic particles via $\rho_\nu = \frac{7}{8}(4/11)^{4/3}\rho_\gamma N_{\rm eff}$. Here ρ_ν and ρ_γ represent the fractional energy density for neutrino and CMB photon, respectively. The entropy transfer between neutrinos and thermal bath modifies this number to $N_{\rm eff} = 3.046$ [48, 49]. However, larger values of $N_{\rm eff}$ are reported by the cosmic observations. Depending on the datasets, constraint results on $N_{\rm eff}$ are qualitatively changed. For instance, it is pointed out that the observational deuterium abundance D/H favors the presence of extra radiation [50, 51]: $N_{\rm eff} = 3.90 \pm 0.44$. The combining analysis of CMB data from the 7-year WMAP and the Atacama Cosmology Telescope (ACT) gives an excess $N_{\rm eff} = 5.3 \pm 1.3$ [52], and the addition of BAO and H_0 data decreases the value $N_{\rm eff} = 4.56 \pm 0.75$ [52, 53]. CMB data from the 9-year WMAP combining with the South Pole Telescope (SPT) and the 3-year Supernova Legacy Survey (SNLS3) provides a non-standard value, $N_{\rm eff} = 3.96 \pm 0.69$ [54, 55]. Ref. [28] shows that $N_{\rm eff} = 3.62^{+0.50}_{-0.48}$ for using the Planck+WP+highL+H_0 and $N_{\rm eff} = 3.52^{+0.48}_{-0.45}$ for using the Planck+WP+highL+BAO+H_0, whose analysis suggests the presence of a dark radiation at 95% confidence level. For more limits on $N_{\rm eff}$, one can see refs. [56–58].

The above urgency to search source of DR is relieved by the study in ref. [6]. Given that $N_{\rm eff}$ is degenerate with the value of H_0, ref. [6] focuses on how the H_0 prior changes the value of $N_{\rm eff}$, and obtains the result that a lower prior for H_0 moves the limits to lower $N_{\rm eff}$. It is pointed out in ref. [6] that there is no longer that much evidence supporting the existence of DR, since this evidence is partially driven by the larger value $H_0 = 73.8 \pm 2.4$ km s^{-1}Mpc^{-1} from the HST while several measurements suggest the lower value of H_0, such as $H_0 = 68 \pm 2.8$ km s^{-1}Mpc^{-1} from the median statistics (MS) analysis of the 537 non-CMB measurements [59], $H_0 = 67.3 \pm 1.2$ km s^{-1}Mpc^{-1} from the Planck+WP+highL [28] and $H_0 = 68.1 \pm 1.1$ km s^{-1}Mpc^{-1} from the 6dF+SDSS+BOSS+WiggleZ BAO data sets [28]. For model-dependent results, ref. [6] shows that in the ΛCDM it indicates the presence of DR with the HST H_0 prior, while there is no significant statistical evidence for existence of DR with the MS H_0 prior [6]; in XCDM parametrization of time-evolving DE it brings the result: the evidence for DR is significant for both the HST H_0 prior and the MS H_0 prior [6].

In this section, we explore the RMCG model that apparent extra DR directly links to the physics of the cosmological-constant (CC) DE. Fixing $A = 1/3$, RMCG fluid unifies the DE and DR, where the Friedmann equation becomes

$$\begin{aligned} H^2(a)/H_0^2 &= \Omega_{0m}a^{-3} + (\Omega_{0\gamma} + \Omega_{0\nu})a^{-4} \\ &\quad + (1 - \Omega_{0m} - \Omega_{0\gamma} - \Omega_{0\nu})[A_s^2 + (1 - A_s)^2 a^{-4} + 2A_s(1 - A_s)a^{-2}] \\ &= \Omega_{0m}a^{-3} + (\Omega_{0\gamma} + \Omega_{0\nu})a^{-4} + \Omega_{01} + \Omega_{02}a^{-4} + \Omega_{03}a^{-2}. \end{aligned} \tag{2.6}$$

Here $\Omega_{01} = (1 - \Omega_{0m} - \Omega_{0\gamma} - \Omega_{0\nu})A_s^2 = \Omega_\Lambda$ is the energy density of cosmological-constant type DE, $\Omega_{02} = (1 - \Omega_{0m} - \Omega_{0\gamma} - \Omega_{0\nu})(1 - A_s)^2 = \Omega_{0dr}$ is the coefficient of DR term that is a characteristic feature in the RMCG (A=1/3) fluid, the term $\Omega_{03}a^{-2} = 2A_s(1 - \Omega_{0m} - \Omega_{0\gamma} - \Omega_{0\nu})(1 - A_s)a^{-2} = \Omega_{0k}^{\rm eff}a^{-2}$ dilutes as a^{-2} jus like the curvature density in the non-flat geometry, called effective curvature density. In the non-flat universe, then the current curvature density is modified as $\Omega_{0k} + \Omega_{0k}^{\rm eff}$. Besides the RMCG fluid, we supplement the matter and radiation components in eq. (2.6).

Eq. (2.6) shows that the dimensionless density parameters (DE, DR and effective curvature density) relate to the RMCG model parameter A_s. The values of these density parameters should be consistent with observations. Given that relativistic particle includes the photon, neutrino and dark radiation, the total dimensionless density parameter of relativistic particle is written as $\Omega_{0r}^{\rm tot} = \Omega_{0\gamma} + \Omega_{0\nu} + \Omega_{0dr} = \Omega_{0\gamma}[1 + \frac{7}{8}(\frac{4}{11})^{4/3}N_{\rm eff}]$, where the photon density parameter $\Omega_{0\gamma} = 2.469 \times 10^{-5}h^{-2}$ [60]. Writing $N_{\rm eff} = N_{\rm eff}^{SM} + \Delta N_{\rm eff}$ and $N_{\rm eff}^{SM} = 3.04$, one reads $\Omega_{0dr} = \frac{7}{8}(\frac{4}{11})^{4/3}\Omega_{0\gamma}\Delta N_{\rm eff}$. On the other hand, in the RMCG (A=1/3) model we receives $\Omega_{0dr} = \Omega_{02} = (1 - \Omega_{0m} - \Omega_{0\gamma} - \Omega_{0\nu})(1 - A_s)^2$. Taking $\Omega_{0m} = 0.3$ and $\Delta N_{\rm eff} = [0.5, 1, 2]$, we can calculate the values of A_s and the dimensionless density parameters, which are listed in table 4. It is found from this table that the values of Ω_Λ and $\Omega_{0k}^{\rm eff}$ are compatible to the cosmic observations [4, 28], where Ω_Λ is around 0.7 and $\Omega_{0k} \sim 0$. And corresponding to $A_s < 1$ (or $A_s > 1$), we have $\Omega_{0k}^{\rm eff} > 0$ (or $\Omega_{0k}^{\rm eff} < 0$).

ΔN_{eff}	A_s	Ω_Λ	Ω_{0k}^{eff}
0.5	0.9972 or 1.0028	0.6920 or 0.7080	0.0079 or -0.0080
1	0.9960 or 1.0040	0.6944 or 0.7056	0.0056 or -0.0056
2	0.9943 or 1.0057	0.6961 or 0.7039	0.0039 or -0.0039

Table 4. Values of A_s, Ω_Λ and Ω_{0k}^{eff} calculated by using the values of ΔN_{eff} and fixing $\Omega_{0m} = 0.3$.

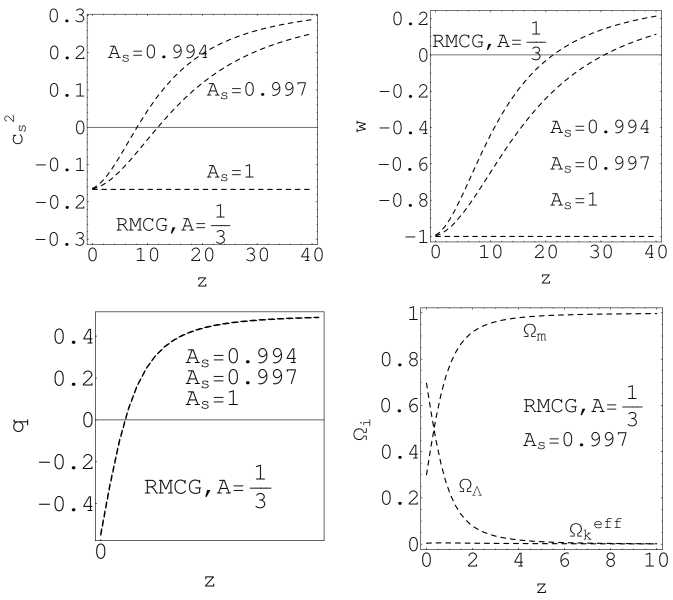

Figure 3. Behaviors of the c_s^2, w, q and Ω_i versus z for the RMCG ($A = 1/3$) unified model of DE and DR.

We plot pictures of the dimensionless density parameters and deceleration parameter versus z. The third picture in figure 3 describes a universe having the transition from decelerated expansion to accelerated expansion. And the evolutions of $q(z)$ are almost the same for taking different value of A_s, due to a small variable region of A_s bounded by ΔN_{eff}. The values of current deceleration parameter and transition redshift are $q_0 = -0.546^{+0.004}_{-0.004}$ and $z_T = 0.668^{+0.003}_{-0.004}$, a narrow range. Figure 3 also illustrates the evolution of $c_s^2(z)$ for the RMCG ($A = 1/3$) fluid, where the positive value of c_s^2 is converted to the negative value with the evolution of universe. Since the RMCG ($A = 1/3$) unified fluid do not include matter, the negative value of c_s^2 will not destroy the structure formation. Just as for the cosmological constant DE, we have $c_s^2 = -1$. The negative c_s^2 for DE is in fact necessary if one requires the negative pressure to produce the accelerating universe. This is not inconsistent with the structure formation. For the behavior of w, at late time we can get $w < 0$ which can be responsibility to the accelerating universe, and at early time we obtain $w \sim 1/3$. According to the analysis above, the behaviors of cosmological quantities in the RMCG ($A = 1/3$) model are accordant with the current observational universe. Then the RMCG ($A = 1/3$) model can be considered as a candidate for the DE and DR. At last, we note that we do not discuss the case of $A_s > 1$ for the RMCG ($A = 1/3$), since the c_s^2 and w will be divergent at some points (when $A_s = -(1 - A_s)a^{-\frac{3}{2}(1+A)}$).

JHEP02(2015)071

2.3 RMCG fluid as dark energy

The unification of the DE and DM (or DR) have been discussed in above parts. In the following, we investigate other possible properties of the RMCG fluid by taking values of A (except $A = 0, 1$ and $1/3$). For $A > 0$ ($A \neq 0, 1, 1/3$), eq. (2.2) states that the RMCG fluid contains the CC and other positive-pressure or negative-pressure components (depending on the concrete value of A). We know nothing about these indeterminate components, such as their function in universe or their responsibility to observations. So, here we do not discuss the case of $A > 0$. For $A < 0$, the RMCG fluid plays a role as the dynamical phantom or dynamical quintessence DE, where the Friedmann equation is written as

$$\begin{aligned} H^2(a)/H_0^2 &= \Omega_{0m}a^{-3} + \Omega_{0r}a^{-4} + \Omega_{0RMCG}\left[A_s^2 + (1-A_s)^2 a^{-3(1+A)} + 2A_s(1-A_s)a^{\frac{-3(1+A)}{2}}\right] \\ &= \Omega_{0m}a^{-3} + \Omega_{0r}a^{-4} + \Omega_{01} + \Omega_{02}a^{-3(1+w_2)} + \Omega_{03}a^{-3(1+w_3)}, \end{aligned} \tag{2.7}$$

where $\Omega_{0RMCG} = 1 - \Omega_{0m} - \Omega_{0r}$, $\Omega_{01} = \Omega_{0RMCG}A_s^2$, $\Omega_{02} = \Omega_{0RMCG}(1-A_s)^2$ and $\Omega_{03} = 2\Omega_{0RMCG}A_s(1-A_s)$. For $A < -1$, we easily get $w_2 = A < -1$ and $w_3 = \frac{A-1}{2} < -1$. So, the RMCG fluid comprises the CC and phantom DE, which plays a role as the phantom-type DE; for $0 > A > -1$, the RMCG fluid includes the CC and quintessence DE; for $A = -1$ or $A_s = 1$, the RMCG fluid reduces to the CC. Since we in theory have $0 \leq A_s \leq 1$ due to the constraint on the current dimensionless density parameter $0 < \Omega_{0j} < 1$, we can get the limit $-1 < A < -1/3$ for the quintessence-type DE; we can obtain the theoretical limit $A < -1$ with $0 < A_s < 1$ for the phantom-type DE. For $A_s > 1$, the phantom-type DE ($-1 < A < 0$) and the quintessence-type DE ($A < -1$) are non-physical, which should be ruled out.

Figure 4 illustrates the dependence of $w(z)$ on model parameters for the RMCG ($A < 0$) fluid. From figure 4, we can read properties of $w(z)$. (1) The CC, quintessence and phantom DE can be realized in this RMCG fluid by taking different values of A and A_s; (2) According to four upper figures in figure 4, for phantom (two upper-right figures) we have the result that the less values of parameters A and A_s, the less value of w. For quintessence (two upper-left figures) we have the results that the less value of parameter A, the less value of w, while the less value of parameter A_s, the larger value of w; (3) As we can see from four upper figures in figure 4, the value of more near to $A = -1$, the less influence on w from A_s. Also, from four lower figures in figure 4, we obtain the result that the value of more near to $A_s = 1$, the less influence on w from A.

Trajectories of $q(z)$ in the RMCG ($A < 0$) model are drew in figure 5, which describe a universe transiting from decelerating expansion to accelerating expansion. One can also see an interesting property for $q(z)$ from figure 5. The behavior of $q(z)$ is almost the same for using the different value of A_s (or A), when the value of another model parameter A (or A_s) is near to -1 (or 1). For example, $q(z)$ is not sensitive to the change of value for A_s (or A), when we take $A = -0.9$ and $A = -1.1$ (or, $A_s = 0.9$ and $A_s = 0.95$). By the way, figure 6 illustrates the evolutions of $c_s^2(z)$ for RMCG ($A < 0$) fluid, where the negative c_s^2 is obtained.

JHEP02(2015)071

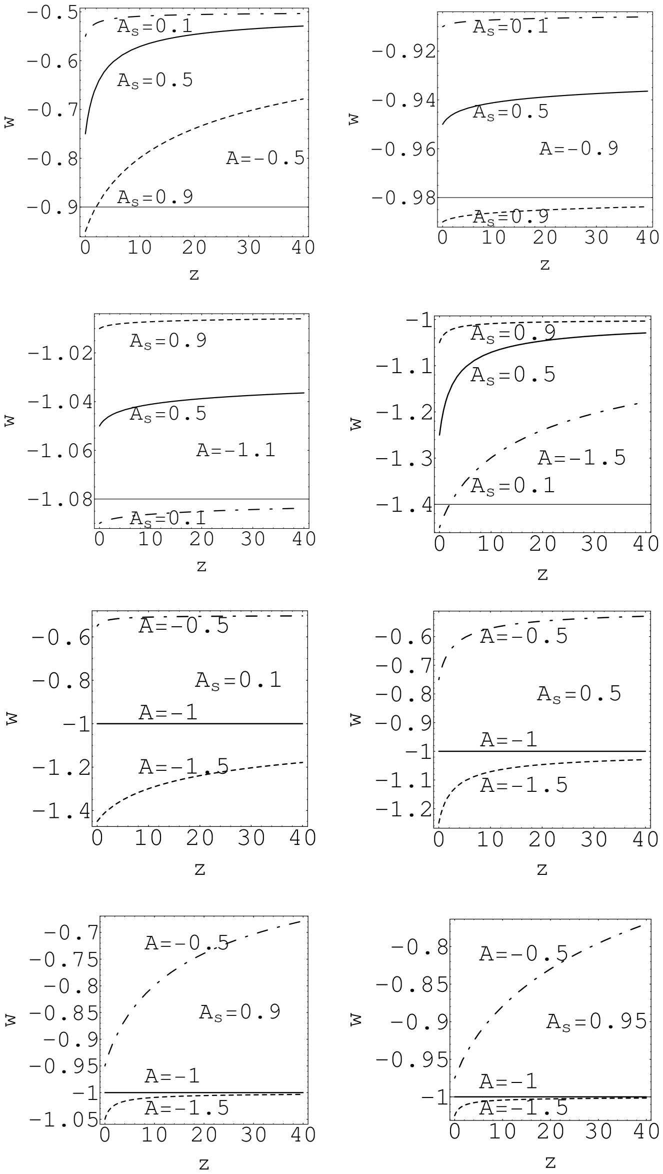

Figure 4. Evolutions of $w(z)$ for the RMCG ($A < 0$) fluid by taking different values of model parameters.

3 Evolutions of growth factor and Hubble parameter in the RMCG and comparisons with cosmic data

Via the cosmic observations, peoples obtain some values of growth factor f [61–68] and Hubble parameter H [69–75], which are listed in table 5 and 6. We apply the f and H to test the RMCG models by comparing them with the observational data. Growth factor is defined as $f \equiv d\ln\delta/d\ln a$, which complies with the following equation

$$\frac{df}{da} + \frac{f^2}{a} + \left[\frac{2}{a} + \frac{(d\ln H)}{da}\right] f - \frac{3\Omega_m(a)}{2} = 0, \tag{3.1}$$

JHEP02(2015)071

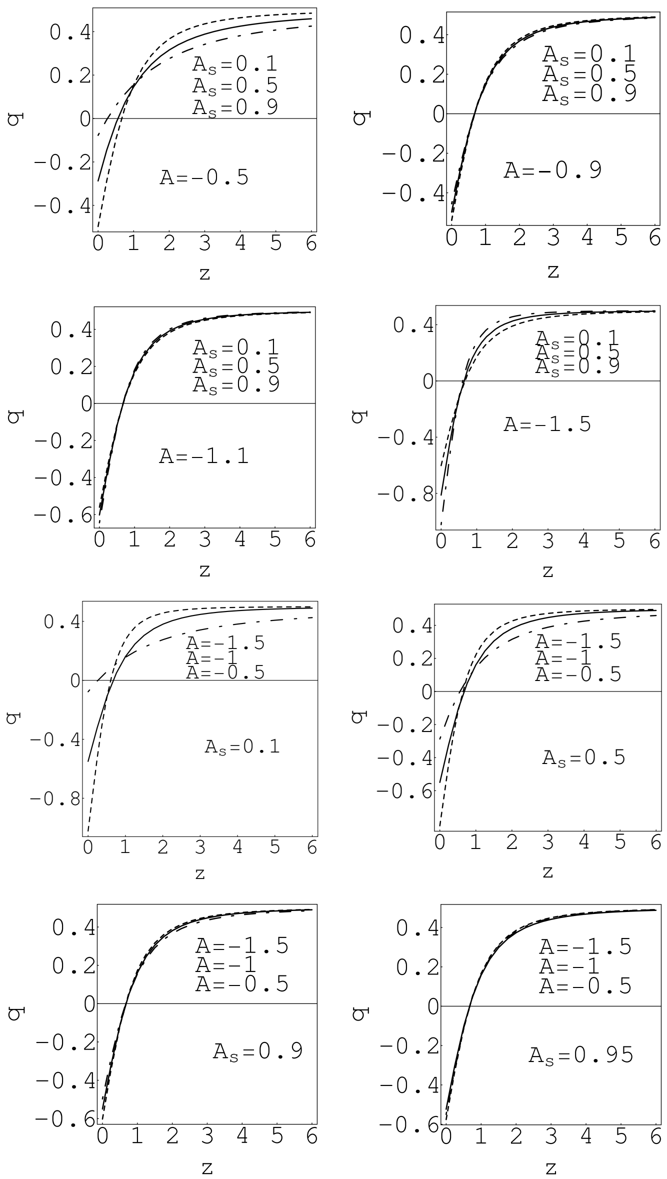

Figure 5. Evolutions of $q(z)$ for the RMCG ($A < 0$) model by taking different values of A and A_s.

Number	1	2	3	4	5	6	7	8	9	10
z	0.15	0.22	0.32	0.35	0.41	0.55	0.60	0.77	0.78	1.4
f	0.51	0.6	0.654	0.7	0.7	0.75	0.73	0.91	0.7	0.9
σ	0.11	0.1	0.18	0.18	0.07	0.18	0.07	0.36	0.08	0.24
ref.	[61, 62]	[63]	[64]	[65]	[63]	[66]	[63]	[67]	[63]	[68]

Table 5. Data of growth factor f with errors at different redshift.

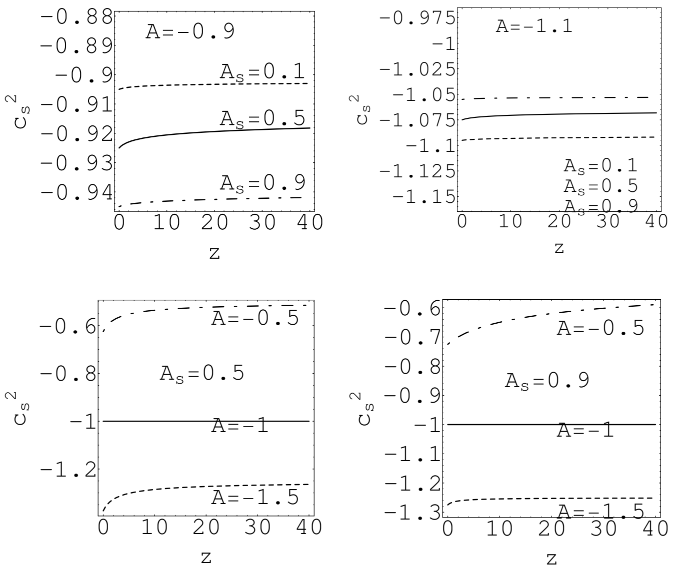

Figure 6. Evolutions of the $c_s^2(z)$ for the RMCG ($A < 0$) fluid by taking different values of model parameters.

Number	1	2	3	4	5	6	7	8	9	10	11	12	13	14	15
z	0.07	0.09	0.10	0.12	0.17	0.179	0.199	0.2	0.27	0.28	0.35	0.352	0.40	0.44	0.48
H	69	69	69	68.6	83	75	75	72.9	77	88.8	76.3	83	95	82.6	97
σ	19.6	12	12	26.2	8	4	5	29.6	14	36.6	5.6	14	17	7.8	62
ref.	[73]	[69]	[69]	[73]	[69]	[71]	[71]	[73]	[69]	[73]	[75]	[71]	[69]	[74]	[70]
Number	16	17	18	19	20	21	22	23	24	25	26	27	28	29	
z	0.593	0.6	0.68	0.73	0.781	0.875	0.88	0.90	1.037	1.30	1.43	1.53	1.75	2.3	
H	104	87.9	92	97.3	105	125	90	117	154	168	177	140	202	224	
σ	13	6.1	8	7.0	12	17	40	23	20	17	18	14	40	8	
ref.	[71]	[74]	[71]	[74]	[71]	[71]	[70]	[69]	[71]	[69]	[69]	[69]	[69]	[72]	

Table 6. $H(z)$ data with errors at different redshift (in units [km s^{-1} Mpc^{-1}]).

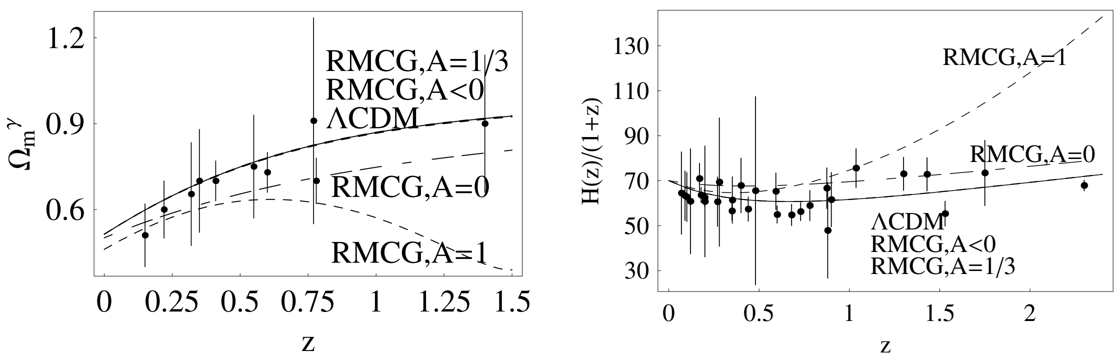

Figure 7. Evolutions of $\Omega_m^\gamma(z)$ and $H(z)/(1+z)$ versus z for the RMCG and ΛCDM model.

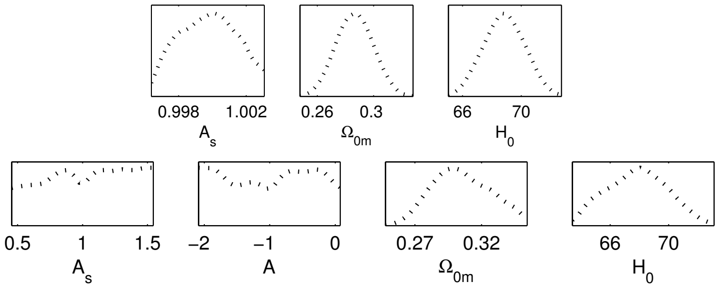

Figure 8. The 1D distribution of model parameters for the RMCG1 (left) and RMCG2 (right) model.

JHEP02(2015)071

deriving by the perturbation equation $\ddot{\delta} + 2H\dot{\delta} - 4\pi G\rho_m\delta = 0$. Here $\delta \equiv \delta\rho_m/\rho_m$ is the matter density contrast and "dot" denotes the derivative with respect to cosmic time t. Usually , it is hard to find the analytical solutions to eq. (3.1). The approximation $f \simeq \Omega_m^\gamma$ has been used in many papers, which provides an excellent fit to the numerical form of $f(z)$ for various cosmological models [76–81]. Growth index γ can be given by considering the zeroth order and the first order terms in the expansion for γ [82], $\gamma = \frac{3(1-w)}{(5-6w)} + \frac{3(1-w)(1-\frac{3}{2}w)(1-\Omega_m)}{125(1-\frac{6w}{5})^3}$. We illustrate the Ω_m^γ versus z in figure 7 by taking $\Omega_{0m} = 0.3$ and $A_s = 0.49$ for the RMCG ($A = 0$), $\Omega_{0m} = 0.3$ and $A_s = 0.84$ for the RMCG ($A = 1$), $\Omega_{0m} = 0.3$ and $A_s = 0.997$ for the RMCG ($A = 1/3$), $\Omega_{0m} = 0.3$, $A_s = 0.95$ and $A = -1.1$ for the RMCG ($A < 0$). It can be seen from figure 7 that the behaviors of $\Omega_m^\gamma(z)$ in the RMCG ($A = 1/3$) and RMCG ($A < 0$) model are almost the same as the popular ΛCDM model (solid line in figure 7), where an increasing function versus z is consistent with the current observations. But, $\Omega_m^\gamma(z)$ in the RMCG ($A = 1$) much deviates from that in the ΛCDM model at the higher redshift. For clarity, we plot the trajectories of $H(z)/(1+z)$ for the discussional models, and compare them with the 29 observational $H(z)$ data listed in table 6. The difference of pictures between the RMCG ($A = 1$) model and ΛCDM model is apparent at high redshift. And at the high redshift, the evolutions of $\Omega_m^\gamma(z)$ and $H(z)/(1+z)$ in the RMCG ($A = 1$) obviously deviate from the observational data. From above, it is shown that the RMCG ($A = 1$) fluid as the unification of dark matter and dark energy is not well accordant with the f data and the Hubble data. But, the RMCG ($A = 1/3$) and RMCG ($A < 0$) model are well consistent with these two cosmic datasets.

4 Parameter evaluation and model comparison

In this section, we investigate the parameter space of the RMCG model. It can be known from the analysis above that the RMCG unified model of the DE and DM are not favored, which have some questions on structure formation. For the RMCG (A=0) unified model, a negative sound speed will introduce the instability at structure formation. For the RMCG (A=1) unified model, perturbation quantity f is not compatible with cosmic data, and a super-deceleration ($q > \frac{1}{2}$) expanded universe is not satisfied with the matter-dominate universe. So, these two cases will not studied in the following. We discuss the cosmic constraint on the RMCG models with $A = 1/3$ (RMCG1) and $A < 0$ (RMCG2). The data we use

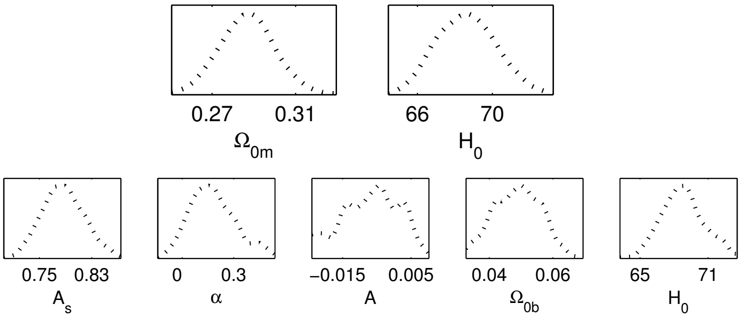

Figure 9. The 1D distribution of model parameters for the ΛCDM (left) and MCG model (right).

Case model	Free parameters	$\chi^2_{\rm min}$	K	ΔAIC
RMCG1 ($A=\frac{1}{3}$)	Ω_{0m}, A_s, H_0, Ω_{0r}	604.976	3	0
ΛCDM	Ω_{0m}, H_0, Ω_{0r}, Ω_{0dr}	604.979	3	0.003
RMCG2 ($A<0$)	Ω_{0m}, A_s, A, H_0, Ω_{0r}, Ω_{0dr}	603.636	5	2.660
MCG	Ω_{0b}, A_s, A, α, H_0, Ω_{0r}, Ω_{0dr}	603.243	6	4.267

Table 7. Information criteria results.

includes: baryon acoustic oscillation (BAO) data from the WiggleZ [83], 2dfGRs [84] and SDSS [85] survey, X-ray cluster gas mass fraction [86], Union2 dataset of type supernovae Ia (SNIa) [87] and 29 Hubble data listed in table 6. The constraint methods are described in appendix. For RMCG1, we have $A_s = 0.9993^{+0.0016+0.0028}_{-0.0016-0.0028}$, $\Omega_{0m} = 0.287^{+0.012+0.024}_{-0.012-0.024}$ and $H_0 = 68.84^{+1.32+2.65}_{-1.32-2.47}$ with 68% and 95% confidence levels. Obviously, A_s is near to 1 and has the small confidence level. This calculation result for A_s is approximatively equal to the cosmic constraint on $\Delta N_{\rm eff} \in (0,1)$, which is consistent with other combining constraints on $N_{\rm eff}$ [28]. By the analysis of error-propagation, we calculate the DE density $\Omega_\Lambda = 0.713^{+0.012+0.024}_{-0.012-0.024}$. For RMCG2, we find that $\Omega_{0m} = 0.297^{+0.015+0.031}_{-0.016-0.028}$ and $H_0 = 68.25^{+1.46+2.92}_{-1.45-3.02}$, while the model parameters A and A_s are not convergent. The results are illustrated in figure 8. From eq. (2.7), we notice tha RMCG2 DE model reduces to the popular CC model by fixing $A=-1$ (or $A_s=1$), whatever value of A_s (or A) is taken. The non-convergent results on A and A_s may be interpreted that the RMCG2 model can not be distinguished from the CC model by the cosmic data used in this paper.

Next we use the objective information criteria (IC) to estimate the quality of above RMCG models. Akaike information criteria (AIC) is defined as [88, 89]

$$AIC = -2\ln\mathcal{L}_{\rm max} + 2K, \tag{4.1}$$

where $\mathcal{L}_{\rm max}$ is the highest likelihood in the model with $-2\ln\mathcal{L}_{\rm max} = \chi^2_{\rm min}$, K is the number of free parameters to interpret the complexity of model. Usually, candidate model which minimizes the AIC is usually considered the best. Comparing with the best one, one can calculate the difference for other model $\Delta{\rm AIC} = \Delta\chi^2_{\rm min} + 2\Delta K$. The rules for judging the strength of models are as follows. For $0 \leq \Delta{\rm AIC}_i \leq 2$, model i almost gains the same data support as the best model; for $2 \leq \Delta{\rm AIC}_i \leq 4$, model i gets the less support; and with $\Delta{\rm AIC}_i > 10$ model i is practically irrelevant [88].

JHEP02(2015)071

Case model	Best-fit z_{da}	Mean with standard deviation
RMCG1 ($A=\frac{1}{3}$)	0.70	0.71 ± 0.03
ΛCDM	0.70	0.71 ± 0.03
RMCG2 ($A<0$)	0.67	0.68 ± 0.03
MCG	0.69	0.68 ± 0.05

Table 8. Values of cosmological deceleration-acceleration transition redshift z_{da}.

Since several observations imply the existence of DR, we take the DR density Ω_{0dr} as an additional free parameter in the ΛCDM, RMCG2 and MCG models. But, Ω_{0dr} is naturally included in the RMCG1 model by the relation between Ω_{0dr} and model parameter A_s and Ω_{0m}. According to the calculation results in table 7, one reads that the best model is the RMCG1. But, the ΛCDM model almost receives the same support as the RMCG1, since they almost have the same AIC values. Comparing with the best RMCG1 model, the ΔAIC values of the RMCG2 and MCG model are calculated, too. From table 7, it is easy to see that the RMCG2 model is less supported by the AIC model-selection method, since $\Delta AIC = 2.660$ at the range from 2 to 4. In addition, though the MCG model has the minimum value of χ^2, it is not favored by analysis of the AIC, as it has the more large value $\Delta AIC = 4.267$ resulted by the more model parameters. Corresponding to the $\chi^2_{\rm min}$ value, the constraint results on free parameters are $\Omega_{0m} = 0.286^{+0.012+0.024}_{-0.012-0.023}$ and $H_0 = 68.57^{+1.31+2.60}_{-1.31-2.43}$ for the ΛCDM model; $A_s = 0.788^{+0.031+0.060}_{-0.028-0.063}$, $\alpha = 0.167^{+0.121+0.236}_{-0.110-0.205}$, $A = -0.0041^{+0.0063+0.0102}_{-0.0060-0.0139}$, $\Omega_{0b} = 0.0501^{+0.0090+0.0160}_{-0.0093-0.0173}$ and $H_0 = 68.46^{+1.55+2.87}_{-1.44-3.01}$ for the MCG model. Using the best-fit model parameters and the covariance matrix, we find that all the four models listed in table 8 show the presence of a cosmological deceleration-acceleration transition. The best-fit values of translation redshift z_{da} are 0.70, 0.70, 0.67 and 0.69 corresponding to the RMCG1, ΛCDM, RMCG2 and MCG model, respectively. The mean with standard deviation are 0.71 ± 0.03, 0.71 ± 0.03, 0.68 ± 0.03 and 0.68 ± 0.05 corresponding to the RMCG1, ΛCDM, RMCG2 and MCG model, respectively. These values are in agreement with the result $z_{da} = 0.74 \pm 0.05$ given by ref. [91].

One can notice that the other criticism mechanism—-Bayesian information criteria (BIC) that is defined as $BIC = -2\ln\mathcal{L}_{\rm max} + K\ln n$ [90] is not studied in this paper. Here n is the number of datapoints in the fitting. As we can see from the BIC definition, the BIC value not only depends on the number of free parameter K and the value of χ^2, but also depends on the number of datapoints n. So, for the same models the different evaluation results would be given by the BIC analysis (induced by the different values of $\ln n$) when one uses the different datapoints. For instance, the value of $\ln n$ is obviously different for case of including or not including SNIa data in combining constraint, since the SNIa data have the large number. Given that the datapoint are always increasing, it seems that the calculation result from BIC is not "fair" for more-parameter model when the more datapoints are given. Quantitatively, the AIC and BIC method can give the same result for $\ln n = 2$ ($n \simeq 7.4$). For datapoints used in our analysis, it has $\ln n = 6.452$. Seeing that the BIC is not "absolutely objective", i.e. its value much depends on the number of datapoints one use, here we do not apply the BIC criticism method to evaluate the RMCG models.

5 Conclusions

The RMCG models are from the subclass of the famous MCG model that has been studied in great detail over the years. But, most of them were studied as a unification of DM and DE in the past. In this paper, we study the RMCG cosmology from a different point of view. We discuss the different cases in which the RMCG is regarded as the DE or the unified model. New interesting physical results are obtained in the RMCG dark models. The results show that (1) the RMCG unified model of the dark energy and dark matter (with model parameter $A = 0$ or $A = 1$) tends to be ruled out by analysing the behaviors of cosmological quantities. For example, the RMCG (A=0) unified model appears a negative sound speed which leads to the instability of the structure formation, growth factor f in the RMCG (A=1) unified model is not consistent with cosmic observational data. In addition, a super-deceleration expanded universe ($q > 1/2$) is not satisfied at the matter-dominate epoch and a radiation-dominate universe will not appear in the RMCG (A=1) model, due to the stiff matter; (2) the RMCG ($A = 1/3$) unified model of the DE and DR is a candidate to interpret the accelerating universe. It produces the good behaviors of cosmological quantities and the good fits to the current observational data: growth factor and Hubble parameter. In addition, it provides an origin of the DE and DR. The energy densities of these two dark components are self-consistent; (3) the RMCG ($A < 0$) fluid as DE also has some attractive features. For example, the CC, quintessence and phontom DE can be realized in the RMCG ($A < 0$) fluid, and in some situations the evolutions of cosmological quantities are not much sensitive to the variation of model-parameters values.

At last, we investigate the parameter space of the RMCG ($A = 1/3$) and RMCG ($A < 0$) model. Fitting the cosmic observational data to the RMCG ($A = 1/3$) model, we obtain the limit on RMCG ($A = 1/3$) model parameter $A_s = 0.9993^{+0.0016+0.0028}_{-0.0016-0.0028}$ at 68% and 95% confidence levels, which are consistent with other constraint result on $\triangle N_{\rm eff} \in (0, 1)$. Meanwhile, the RMCG ($A = 1/3$) model almost has the same support as the most popular ΛCDM model via the AIC calculation. In case of fitting the cosmic data to the RMCG ($A < 0$) model, model parameters A and A_s are not convergent. The theoretical predictions on the RMCG ($A < 0$) model parameters are $0 < A_s < 1$ with $-1 < A < -1/3$ for the quintessence DE, and $0 < A_s < 1$ with $A < -1$ for the phantom DE. But by the analysis of AIC, the RMCG ($A < 0$) model has the less support from the observational data.

Acknowledgments

Authors thank the Dr. Yuting Wang for improving the English of this paper. The research work is supported by the National Natural Science Foundation of China (11205078,11275035,11175077).

A Cosmic data and constraint methods

In the following we introduce the cosmic data used in this paper, including the BAO, $f_{\rm gas}$, SNIa and H(z) data. Theoretically, one can define three distance parameter. $D_A(z)$ is the proper angular diameter distance

$$D_A(z) = \frac{c}{(1+z)\sqrt{|\Omega_k|}} \mathrm{sinn}\left[\sqrt{|\Omega_k|}\int_0^z \frac{dz'}{H(z')}\right], \tag{A.1}$$

which relates to other two distance quantities D_L and D_V by

$$D_L(z) = \frac{H_0}{c}(1+z)^2 D_A(z) \tag{A.2}$$

$$D_V(z) = \left[(1+z)^2 D_A^2(z)\frac{cz}{H(z;p_s)}\right]^{1/3} = H_0\left[\frac{z}{E(z;p_s)}\left(\int_0^z \frac{dz^{'}}{E(z^{'};p_s)}\right)^2\right]^{\frac{1}{3}}. \tag{A.3}$$

Here p_s is the theoretical model parameters, $sinn(\sqrt{|\Omega_k|}x)$ denotes $\sin(\sqrt{|\Omega_k|}x)$, $\sqrt{|\Omega_k|}x$ and $\sinh(\sqrt{|\Omega_k|}x)$ for $\Omega_k < 0$, $\Omega_k = 0$ and $\Omega_k > 0$, respectively.

A.1 BAO

BAO data can be extracted from the WiggleZ Dark Energy Survey (WDWS) [83], the Two Degree Field Galaxy Redshift Survey (2dFGRS) [84] and the Sloan Digitial Sky Survey (SDSS) [85]. One can construct

$$\chi^2_{BAO}(p_s) = X^t V^{-1} X, \tag{A.4}$$

with

$$V^{-1} = \begin{pmatrix} 4444 & 0 & 0 & 0 & 0 & 0 \\ 0 & 30318 & -17312 & 0 & 0 & 0 \\ 0 & -17312 & 87046 & 0 & 0 & 0 \\ 0 & 0 & 0 & 23857 & -22747 & 10586 \\ 0 & 0 & 0 & -22747 & 128729 & -59907 \\ 0 & 0 & 0 & 10586 & -59907 & 125536 \end{pmatrix}, X = \begin{pmatrix} \frac{r_s(z_d)}{D_V(0.106)} - 0.336 \\ \frac{r_s(z_d)}{D_V(0.2)} - 0.1905 \\ \frac{r_s(z_d)}{D_V(0.35)} - 0.1097 \\ \frac{r_s(z_d)}{D_V(0.44)} - 0.0916 \\ \frac{r_s(z_d)}{D_V(0.6)} - 0.0726 \\ \frac{r_s(z_d)}{D_V(0.73)} - 0.0592 \end{pmatrix}. \tag{A.5}$$

V^{-1} is the inverse covariance matrix [85, 92]. X is a column vector which is given by theoretical values minus observational values, and X^t denotes its transpose. $r_s(z) = c\int_0^t \frac{c_s dt}{a} = \frac{c}{\sqrt{3}}\int_0^{1/(1+z)} \frac{da}{a^2 H(a)\sqrt{1+3a\Omega_{0b}/(4\Omega_\gamma)}}$ is the comoving sound horizon size. $c_s^{-2} = 3+\frac{4}{3}\times(\frac{\Omega_{0b}}{\Omega_\gamma})a$ is the sound speed of the photon$-$baryon fluid with $\Omega_\gamma = 2.469\times10^{-5}h^{-2}$. z_d denotes the drag epoch (where baryons were released from photons), $z_d = \frac{1291(\Omega_{0m}h^2)^{-0.419}}{1+0.659(\Omega_{0m}h^2)^{0.828}}[1+b_1(\Omega_{0b}h^2)^{b_2}]$ with $b_1 = 0.313(\Omega_{0m}h^2)^{-0.419}[1+0.607(\Omega_{0m}h^2)^{0.674}]$ and $b_2 = 0.238(\Omega_{0m}h^2)^{0.223}$. h is a re-normalized quantity defined by the Hubble constant $H_0 = 100h$ km s^{-1}Mpc^{-1}.

A.2 X-ray gas mass fraction

In observation of the X-ray gas mass fraction, one can define a parameter [86],

$$f_{\mathrm{gas}}^{\Lambda CDM}(z) = \frac{KA\gamma b(z)}{1+s(z)}\left(\frac{\Omega_{0b}}{\Omega_{0m}}\right)\left[\frac{D_A^{\Lambda CDM}(z)}{D_A(z)}\right]^{1.5} \tag{A.6}$$

for the reference model ΛCDM. Here $A = \left(\frac{H(z)D_A(z)}{[H(z)D_A(z)]^{\Lambda CDM}}\right)^\eta$ is the angular correction factor. $\eta = 0.214 \pm 0.022$ is the slope of the $f_{\rm gas}(r/r_{2500})$ data [86]. Parameter γ denotes permissible departures from the assumption of hydrostatic equilibrium, due to non-thermal pressure support. Bias factor $b(z) = b_0(1 + \alpha_b z)$ accounts for uncertainties in the cluster depletion factor. $s(z) = s_0(1+\alpha_s z)$ accounts for uncertainties of the baryonic mass fraction in stars, and a Gaussian prior for s_0 is employed with $s_0 = (0.16\pm0.05)h_{70}^{0.5}$ [86]. Factor K is utilized to describe the combining effects of the residual uncertainties, and a Gaussian prior $K = 1.0\pm0.1$ is used [86]. Adopting the datapoints published in ref. [86] and following the method introduced in refs. [86], we can constrain theoretical model by calculating

$$\chi^2_{f_{\rm gas}} = \sum_{i=1}^{42} \frac{[f_{\rm gas}^{\Lambda CDM}(z_i) - f_{\rm gas}(z_i)]^2}{\sigma^2_{f_{\rm gas}}(z_i)} + \frac{(s_0 - 0.16)^2}{0.0016^2} + \frac{(K - 1.0)^2}{0.01^2} + \frac{(\eta - 0.214)^2}{0.022^2}, \quad \text{(A.7)}$$

where $\sigma_{f_{\rm gas}}(z_i)$ is the statistical uncertainties. As pointed out in [86], the acquiescent systematic uncertainties have been considered via the parameters η, $b(z)$, $s(z)$ and K.

A.3 SNIa

Cosmic constraint from SNIa observation can be determined by calculating [93–103]

$$\chi^2_{\rm SNIa}(p_s) \equiv \sum_{i=1}^{557} \frac{\{\mu_{\rm th}(p_s, z_i) - \mu_{\rm obs}(z_i)\}^2}{\sigma^2_{\mu_i}}. \quad \text{(A.8)}$$

Here $\mu_{\rm obs}(z_i)$ is the observational distance moduli which can be given by SNIa observation datasets [87], $\mu_{th}(z) = 5\log_{10}[D_L(z)] + \mu_0$ is the theoretical distance modulus with $\mu_0 = 5log_{10}(\frac{H_0^{-1}}{Mpc})+25 = 42.38-5log_{10}h$, and $D_L(z)$ denotes the Hubble-free luminosity distance.

A.4 H(z) data

Using the H(z) data listed in table 6, we can determine the model parameters by minimizing [104–111]

$$\chi^2_H(H_0, p_s) = \sum_{i=1}^{29} \frac{[H_{\rm th}(H_0, p_s; z_i) - H_{\rm obs}(z_i)]^2}{\sigma^2_H(z_i)}, \quad \text{(A.9)}$$

where H_{th} is the theoretical value and $H_{\rm obs}$ is the observational value for the Hubble parameter.

References

[1] V.C. Rubin, N. Thonnard and J. Ford, W. K., *Rotational properties of 21 SC galaxies with a large range of luminosities and radii, from NGC 4605 /R = 4kpc/ to UGC 2885 /R = 122 kpc/*, Astrophys. J. **238** (1980) 471 [INSPIRE].

[2] Supernova Search Team collaboration, A.G. Riess et al., *Observational evidence from supernovae for an accelerating universe and a cosmological constant*, *Astron. J.* **116** (1998) 1009 [astro-ph/9805201] [INSPIRE].

[3] Supernova Cosmology Project collaboration, S. Perlmutter et al., *Measurements of Omega and Lambda from 42 high redshift supernovae*, *Astrophys. J.* **517** (1999) 565 [astro-ph/9812133] [INSPIRE].

[4] WMAP collaboration, C.L. Bennett et al., *Nine-Year Wilkinson Microwave Anisotropy Probe (WMAP) Observations: Final Maps and Results*, *Astrophys. J. Suppl.* **208** (2013) 20 [arXiv:1212.5225] [INSPIRE].

[5] WMAP collaboration, G. Hinshaw et al., *Nine-Year Wilkinson Microwave Anisotropy Probe (WMAP) Observations: Cosmological Parameter Results*, *Astrophys. J. Suppl.* **208** (2013) 19 [arXiv:1212.5226] [INSPIRE].

[6] E. Calabrese, M. Archidiacono, A. Melchiorri and B. Ratra, *The impact of a new median statistics H_0 prior on the evidence for dark radiation*, *Phys. Rev.* **D 86** (2012) 043520 [arXiv:1205.6753] [INSPIRE].

[7] G. Bertone, D. Hooper and J. Silk, *Particle dark matter: Evidence, candidates and constraints*, *Phys. Rept.* **405** (2005) 279 [hep-ph/0404175] [INSPIRE].

[8] CDMS-II collaboration, Z. Ahmed et al., *Dark Matter Search Results from the CDMS II Experiment*, *Science* **327** (2010) 1619 [arXiv:0912.3592] [INSPIRE].

[9] B. Ratra and P.J.E. Peebles, *Cosmological Consequences of a Rolling Homogeneous Scalar Field*, *Phys. Rev.* **D 37** (1988) 3406 [INSPIRE].

[10] R.-G. Cai, *A Dark Energy Model Characterized by the Age of the Universe*, *Phys. Lett.* **B 657** (2007) 228 [arXiv:0707.4049] [INSPIRE].

[11] B. Feng, X.-L. Wang and X.-M. Zhang, *Dark energy constraints from the cosmic age and supernova*, *Phys. Lett.* **B 607** (2005) 35 [astro-ph/0404224] [INSPIRE].

[12] M. Li, *A Model of holographic dark energy*, *Phys. Lett.* **B 603** (2004) 1 [hep-th/0403127] [INSPIRE].

[13] Y. Wang and L. Xu, *Current Observational Constraints to Holographic Dark Energy Model with New Infrared cut-off via Markov Chain Monte Carlo Method*, *Phys. Rev.* **D 81** (2010) 083523 [arXiv:1004.3340] [INSPIRE].

[14] A.Y. Kamenshchik, U. Moschella and V. Pasquier, *An Alternative to quintessence*, *Phys. Lett.* **B 511** (2001) 265 [gr-qc/0103004] [INSPIRE].

[15] Z.-H. Zhu, *Generalized Chaplygin gas as a unified scenario of dark matter/energy: Observational constraints*, *Astron. Astrophys.* **423** (2004) 421 [astro-ph/0411039] [INSPIRE].

[16] A. Pavlov, S. Westmoreland, K. Saaidi and B. Ratra, *Nonflat time-variable dark energy cosmology*, *Phys. Rev.* **D 88** (2013) 123513 [arXiv:1307.7399] [INSPIRE].

[17] C. Feng, B. Wang, Y. Gong and R.-K. Su, *Testing the viability of the interacting holographic dark energy model by using combined observational constraints*, *JCAP* **09** (2007) 005 [arXiv:0706.4033] [INSPIRE].

[18] C. Gao, X. Chen and Y.-G. Shen, *A Holographic Dark Energy Model from Ricci Scalar Curvature*, *Phys. Rev.* **D 79** (2009) 043511 [arXiv:0712.1394] [INSPIRE].

JHEP02(2015)071

[19] J. Lu, E.N. Saridakis, M.R. Setare and L. Xu, *Observational constraints on holographic dark energy with varying gravitational constant*, *JCAP* **03** (2010) 031 [arXiv:0912.0923] [INSPIRE].

[20] C.-J. Feng, *Statefinder Diagnosis for Ricci Dark Energy*, *Phys. Lett.* **B 670** (2008) 231 [arXiv:0809.2502] [INSPIRE].

[21] J.B. Lu, et al., *Revisiting the vacuum energy scenario from the renormalization group method of the QFT theory*, *Eur. Phys. J. Plus* **129** (2014) 27.

[22] J. Hasenkamp and J. Kersten, *Dark radiation from particle decay: cosmological constraints and opportunities*, *JCAP* **08** (2013) 024 [arXiv:1212.4160] [INSPIRE].

[23] J.-F. Zhang, Y.-H. Li and X. Zhang, *Measuring growth index in a universe with sterile neutrinos*, *Phys. Lett.* **B 739** (2014) 102 [arXiv:1408.4603] [INSPIRE].

[24] U. França, R.A. Lineros, J. Palacio and S. Pastor, *Probing interactions within the dark matter sector via extra radiation contributions*, *Phys. Rev.* **D 87** (2013) 123521 [arXiv:1303.1776] [INSPIRE].

[25] S. Dutta and E.N. Saridakis, *Observational constraints on Hořava-Lifshitz cosmology*, *JCAP* **01** (2010) 013 [arXiv:0911.1435] [INSPIRE].

[26] A. Ali, S. Dutta, E.N. Saridakis and A.A. Sen, *Hořava-Lifshitz cosmology with generalized Chaplygin gas*, *Gen. Rel. Grav.* **44** (2012) 657 [arXiv:1004.2474] [INSPIRE].

[27] K. Ichiki, M. Yahiro, T. Kajino, M. Orito and G.J. Mathews, *Observational constraints on dark radiation in brane cosmology*, *Phys. Rev.* **D 66** (2002) 043521 [astro-ph/0203272] [INSPIRE].

[28] Planck collaboration, P.A.R. Ade et al., *Planck 2013 results. XVI. Cosmological parameters*, *Astron. Astrophys.* **571** (2014) A16 [arXiv:1303.5076] [INSPIRE].

[29] M.C. Bento, O. Bertolami and A.A. Sen, *Generalized Chaplygin gas, accelerated expansion and dark energy matter unification*, *Phys. Rev.* **D 66** (2002) 043507 [gr-qc/0202064] [INSPIRE].

[30] L. Xu, J. Lu and Y. Wang, *Revisiting Generalized Chaplygin Gas as a Unified Dark Matter and Dark Energy Model*, *Eur. Phys. J.* **C 72** (2012) 1883 [arXiv:1204.4798] [INSPIRE].

[31] J.B. Lu et al., *Comparing the VGCG model as the unification of dark sectors with observations*, *Sci. China Phys. Mech. Astron.* **57** (2014) 796.

[32] J.C. Fabris, T.C.C. Guio, M. Hamani Daouda and O.F. Piattella, *Scalar models for the generalized Chaplygin gas and the structure formation constraints*, *Grav. Cosmol.* **17** (2011) 259 [arXiv:1011.0286] [INSPIRE].

[33] H.B. Benaoum, *Accelerated universe from modified Chaplygin gas and tachyonic fluid*, hep-th/0205140 [INSPIRE].

[34] J.C. Fabris, H.E.S. Velten, C. Ogouyandjou and J. Tossa, *Ruling out the Modified Chaplygin Gas Cosmologies*, *Phys. Lett.* **B 694** (2011) 289 [arXiv:1007.1011] [INSPIRE].

[35] J.D. Barrow, *graduated inflationary universes*, *Phys. Lett.* **B 235** (1990) 40 [INSPIRE].

[36] S. del Campo and R. Herrera, *Tachyon-Chaplygin inflationary universe model*, *Phys. Lett.* **B 660** (2008) 282 [arXiv:0801.3251] [INSPIRE].

[37] R. Herrera, *Chaplygin inflation on the brane*, *Phys. Lett.* **B 664** (2008) 149 [arXiv:0805.1005] [INSPIRE].

JHEP02(2015)071

[38] R. Herrera, *Tachyon-Chaplygin inflation on the brane*, *Gen. Rel. Grav.* **41** (2009) 1259 [arXiv:0810.1074] [INSPIRE].

[39] M.L. Bedran, V. Soares and M.E. Araujo, *Temperature evolution of the FRW universe filled with modified Chaplygin gas*, *Phys. Lett.* **B 659** (2008) 462 [INSPIRE].

[40] J. Lu, L. Xu, H. Tan and S. Gao, *Extended Chaplygin gas as a unified fluid of dark components in varying gravitational constant theory*, *Phys. Rev.* **D 89** (2014) 063526 [INSPIRE].

[41] B.C. Paul, P. Thakur and A. Saha, *Modified Chaplygin Gas as Scalar Field and Holographic Dark Energy Model*, arXiv:0809.3491 [INSPIRE].

[42] S. Silva e Costa, M. Ujevic and A. Ferreira dos Santos, *A Mathematical analysis of the evolution of perturbations in a modified Chaplygin gas model*, *Gen. Rel. Grav.* **40** (2008) 1683 [gr-qc/0703140] [INSPIRE].

[43] S. Ghose, P. Thakur and B.C. Paul, *Observational Constraints on the Model Parameters of a Class of Emergent Universe*, *Mon. Not. Roy. Astron. Soc.* **421** (2012) 20 [arXiv:1105.3303] [INSPIRE].

[44] B.C. Paul, S. Ghose and P. Thakur, *Emergent Universe from A Composition of Matter, Exotic Matter and Dark Energy*, *Mon. Not. Roy. Astron. Soc.* **413** (2011) 686 [arXiv:1101.1360] [INSPIRE].

[45] B.C. Paul, P. Thakur and S. Ghose, *Constraints on Exotic Matter for An Emergent Universe*, *Mon. Not. Roy. Astron. Soc.* **407** (2010) 415 [arXiv:1004.4256] [INSPIRE].

[46] S. Mukherjee, B.C. Paul, N.K. Dadhich, S.D. Maharaj and A. Beesham, *Emergent Universe with Exotic Matter*, *Class. Quant. Grav.* **23** (2006) 6927 [gr-qc/0605134] [INSPIRE].

[47] G.-B. Zhao, J.-Q. Xia, M. Li, B. Feng and X. Zhang, *Perturbations of the quintom models of dark energy and the effects on observations*, *Phys. Rev.* **D 72** (2005) 123515 [astro-ph/0507482] [INSPIRE].

[48] G. Mangano, A. Melchiorri, O. Mena, G. Miele and A. Slosar, *Present bounds on the relativistic energy density in the Universe from cosmological observables*, *JCAP* **03** (2007) 006 [astro-ph/0612150] [INSPIRE].

[49] E. Calabrese, D. Huterer, E.V. Linder, A. Melchiorri and L. Pagano, *Limits on Dark Radiation, Early Dark Energy and Relativistic Degrees of Freedom*, *Phys. Rev.* **D 83** (2011) 123504 [arXiv:1103.4132] [INSPIRE].

[50] K.M. Nollett and G.P. Holder, *An analysis of constraints on relativistic species from primordial nucleosynthesis and the cosmic microwave background*, arXiv:1112.2683 [INSPIRE].

[51] J. Hamann, S. Hannestad, G.G. Raffelt, I. Tamborra and Y.Y.Y. Wong, *Cosmology seeking friendship with sterile neutrinos*, *Phys. Rev. Lett.* **105** (2010) 181301 [arXiv:1006.5276] [INSPIRE].

[52] O.E. Bjaelde, S. Das and A. Moss, *Origin of Delta N_{eff} as a Result of an Interaction between Dark Radiation and Dark Matter*, *JCAP* **10** (2012) 017 [arXiv:1205.0553] [INSPIRE].

[53] J. Dunkley, R. Hlozek, J. Sievers, V. Acquaviva, P.A.R. Ade et al., *The Atacama Cosmology Telescope: Cosmological Parameters from the 2008 Power Spectra*, *Astrophys. J.* **739** (2011) 52 [arXiv:1009.0866] [INSPIRE].

JHEP02(2015)071

[54] M. Archidiacono, E. Giusarma, A. Melchiorri and O. Mena, *Neutrino and dark radiation properties in light of recent CMB observations*, *Phys. Rev.* **D 87** (2013) 103519 [arXiv:1303.0143] [INSPIRE].

[55] C. Kelso, S. Profumo and F.S. Queiroz, *Nonthermal WIMPs as "Dark Radiation" in Light of ATACAMA, SPT, WMAP9 and Planck*, *Phys. Rev.* **D 88** (2013) 023511 [arXiv:1304.5243] [INSPIRE].

[56] M. Archidiacono, E. Giusarma, S. Hannestad and O. Mena, *Cosmic dark radiation and neutrinos*, *Adv. High Energy Phys.* **2013** (2013) 191047 [arXiv:1307.0637] [INSPIRE].

[57] M. Archidiacono, E. Calabrese and A. Melchiorri, *The Case for Dark Radiation*, *Phys. Rev.* **D 84** (2011) 123008 [arXiv:1109.2767] [INSPIRE].

[58] R. Keisler, C.L. Reichardt, K.A. Aird, B.A. Benson, L.E. Bleem et al., *A Measurement of the Damping Tail of the Cosmic Microwave Background Power Spectrum with the South Pole Telescope*, *Astrophys. J.* **743** (2011) 28 [arXiv:1105.3182] [INSPIRE].

[59] G. Chen and B. Ratra, *Median statistics and the Hubble constant*, *Publ. Astron. Soc. Pac.* **123** (2011) 1127 [arXiv:1105.5206] [INSPIRE].

[60] WMAP collaboration, E. Komatsu et al., *Seven-Year Wilkinson Microwave Anisotropy Probe (WMAP) Observations: Cosmological Interpretation*, *Astrophys. J. Suppl.* **192** (2011) 18 [arXiv:1001.4538] [INSPIRE].

[61] E. Hawkins, S. Maddox, S. Cole, D. Madgwick, P. Norberg et al., *The 2dF Galaxy Redshift Survey: Correlation functions, peculiar velocities and the matter density of the universe*, *Mon. Not. Roy. Astron. Soc.* **346** (2003) 78 [astro-ph/0212375] [INSPIRE].

[62] L. Verde, A.F. Heavens, W.J. Percival, S. Matarrese, C.M. Baugh et al., *The 2dF Galaxy Redshift Survey: The Bias of galaxies and the density of the Universe*, *Mon. Not. Roy. Astron. Soc.* **335** (2002) 432 [astro-ph/0112161] [INSPIRE].

[63] C. Blake, S. Brough, M. Colless, C. Contreras, W. Couch et al., *The WiggleZ Dark Energy Survey: the growth rate of cosmic structure since redshift z=0.9*, *Mon. Not. Roy. Astron. Soc.* **415** (2011) 2876 [arXiv:1104.2948] [INSPIRE].

[64] R. Reyes, R. Mandelbaum, U. Seljak, T. Baldauf, J.E. Gunn et al., *Confirmation of general relativity on large scales from weak lensing and galaxy velocities*, *Nature* **464** (2010) 256 [arXiv:1003.2185] [INSPIRE].

[65] SDSS collaboration, M. Tegmark et al., *Cosmological Constraints from the SDSS Luminous Red Galaxies*, *Phys. Rev.* **D 74** (2006) 123507 [astro-ph/0608632] [INSPIRE].

[66] N.P. Ross, J. da Angela, T. Shanks, D.A. Wake, R.D. Cannon et al., *The 2dF-SDSS LRG and QSO Survey: The 2-Point Correlation Function and Redshift-Space Distortions*, *Mon. Not. Roy. Astron. Soc.* **381** (2007) 573 [astro-ph/0612400] [INSPIRE].

[67] L. Guzzo, M. Pierleoni, B. Meneux, E. Branchini, O.L. Fevre et al., *A test of the nature of cosmic acceleration using galaxy redshift distortions*, *Nature* **451** (2008) 541 [arXiv:0802.1944] [INSPIRE].

[68] J. da Angela, T. Shanks, S.M. Croom, P. Weilbacher, R.J. Brunner et al., *The 2dF-SDSS LRG and QSO Survey: QSO clustering and the L-z degeneracy*, *Mon. Not. Roy. Astron. Soc.* **383** (2008) 565 [astro-ph/0612401] [INSPIRE].

[69] J. Simon, L. Verde and R. Jimenez, *Constraints on the redshift dependence of the dark energy potential*, *Phys. Rev.* **D 71** (2005) 123001 [astro-ph/0412269] [INSPIRE].

[70] D. Stern, R. Jimenez, L. Verde, M. Kamionkowski and S.A. Stanford, *Cosmic Chronometers: Constraining the Equation of State of Dark Energy. I: H(z) Measurements*, JCAP **02** (2010) 008 [arXiv:0907.3149] [INSPIRE].

[71] M. Moresco, A. Cimatti, R. Jimenez, L. Pozzetti, G. Zamorani et al., *Improved constraints on the expansion rate of the Universe up to $z \sim 1.1$ from the spectroscopic evolution of cosmic chronometers*, JCAP **08** (2012) 006 [arXiv:1201.3609] [INSPIRE].

[72] N.G. Busca, T. Delubac, J. Rich, S. Bailey, A. Font-Ribera et al., *Baryon Acoustic Oscillations in the Ly-α forest of BOSS quasars*, Astron. Astrophys. **552** (2013) A96 [arXiv:1211.2616] [INSPIRE].

[73] C. Zhang, H. Zhang, S. Yuan, T.-J. Zhang and Y.-C. Sun, *Four new observational $H(z)$ data from luminous red galaxies in the Sloan Digital Sky Survey data release seven*, Res. Astron. Astrophys. **14** (2014) 1221 [arXiv:1207.4541] [INSPIRE].

[74] C. Blake, S. Brough, M. Colless, C. Contreras, W. Couch et al., *The WiggleZ Dark Energy Survey: Joint measurements of the expansion and growth history at $z < 1$*, Mon. Not. Roy. Astron. Soc. **425** (2012) 405 [arXiv:1204.3674] [INSPIRE].

[75] C.-H. Chuang and Y. Wang, *Modeling the Anisotropic Two-Point Galaxy Correlation Function on Small Scales and Improved Measurements of $H(z)$, $D_A(z)$ and $\beta(z)$ from the Sloan Digital Sky Survey DR7 Luminous Red Galaxies*, Mon. Not. Roy. Astron. Soc. **435** (2013) 255 [arXiv:1209.0210] [INSPIRE].

[76] Y. Gong, *The growth factor parameterization and modified gravity*, Phys. Rev. **D 78** (2008) 123010 [arXiv:0808.1316] [INSPIRE].

[77] P. Wu, H.W. Yu and X. Fu, *A Parametrization for the growth index of linear matter perturbations*, JCAP **06** (2009) 019 [arXiv:0905.3444] [INSPIRE].

[78] X. Fu, P. Wu and H. Yu, *The growth of matter perturbations in f(T) gravity*, Int. J. Mod. Phys. **D 20** (2011) 1301 [arXiv:1204.2333] [INSPIRE].

[79] X.-y. Fu, P.-x. Wu and H.-w. Yu, *The Growth of linear perturbations in the DGP model*, Phys. Lett. **B 677** (2009) 12 [arXiv:0905.1735] [INSPIRE].

[80] S. Nesseris and L. Perivolaropoulos, *Testing Lambda CDM with the Growth Function delta(a): Current Constraints*, Phys. Rev. **D 77** (2008) 023504 [arXiv:0710.1092] [INSPIRE].

[81] Y. Gong, M. Ishak and A. Wang, *Growth factor parametrization in curved space*, Phys. Rev. **D 80** (2009) 023002 [arXiv:0903.0001] [INSPIRE].

[82] L.-M. Wang and P.J. Steinhardt, *Cluster abundance constraints on quintessence models*, Astrophys. J. **508** (1998) 483 [astro-ph/9804015] [INSPIRE].

[83] C. Blake, E. Kazin, F. Beutler, T. Davis, D. Parkinson et al., *The WiggleZ Dark Energy Survey: mapping the distance-redshift relation with baryon acoustic oscillations*, Mon. Not. Roy. Astron. Soc. **418** (2011) 1707 [arXiv:1108.2635] [INSPIRE].

[84] F. Beutler, C. Blake, M. Colless, D.H. Jones, L. Staveley-Smith et al., *The 6dF Galaxy Survey: Baryon Acoustic Oscillations and the Local Hubble Constant*, Mon. Not. Roy. Astron. Soc. **416** (2011) 3017 [arXiv:1106.3366] [INSPIRE].

[85] SDSS collaboration, W.J. Percival et al., *Baryon Acoustic Oscillations in the Sloan Digital Sky Survey Data Release 7 Galaxy Sample*, Mon. Not. Roy. Astron. Soc. **401** (2010) 2148 [arXiv:0907.1660] [INSPIRE].

JHEP02(2015)071

[86] S.W. Allen, D.A. Rapetti, R.W. Schmidt, H. Ebeling, G. Morris et al., *Improved constraints on dark energy from Chandra X-ray observations of the largest relaxed galaxy clusters*, *Mon. Not. Roy. Astron. Soc.* **383** (2008) 879 [arXiv:0706.0033] [INSPIRE].

[87] R. Amanullah, C. Lidman, D. Rubin, G. Aldering, P. Astier et al., *Spectra and Light Curves of Six Type Ia Supernovae at* $0.511 < z < 1.12$ *and the Union2 Compilation*, *Astrophys. J.* **716** (2010) 712 [arXiv:1004.1711] [INSPIRE].

[88] M. Biesiada, *Information-theoretic model selection applied to supernovae data*, *JCAP* **02** (2007) 003 [astro-ph/0701721] [INSPIRE].

[89] D. Parkinson, S. Tsujikawa, B.A. Bassett and L. Amendola, *Testing for double inflation with WMAP*, *Phys. Rev.* **D 71** (2005) 063524 [astro-ph/0409071] [INSPIRE].

[90] A.R. Liddle, *How many cosmological parameters?*, *Mon. Not. Roy. Astron. Soc.* **351** (2004) L49 [astro-ph/0401198] [INSPIRE].

[91] O. Farooq and B. Ratra, *Hubble parameter measurement constraints on the cosmological deceleration-acceleration transition redshift*, *Astrophys. J.* **766** (2013) L7 [arXiv:1301.5243] [INSPIRE].

[92] S. Nesseris and J. García-Bellido, *A new perspective on Dark Energy modeling via Genetic Algorithms*, *JCAP* **11** (2012) 033 [arXiv:1205.0364] [INSPIRE].

[93] S. Nesseris and L. Perivolaropoulos, *Comparison of the legacy and gold snia dataset constraints on dark energy models*, *Phys. Rev.* **D 72** (2005) 123519 [astro-ph/0511040] [INSPIRE].

[94] V. Acquaviva and L. Verde, *Observational signatures of Jordan-Brans-Dicke theories of gravity*, *JCAP* **12** (2007) 001 [arXiv:0709.0082] [INSPIRE].

[95] R.-G. Cai, Z.-L. Tuo, Y.-B. Wu and Y.-Y. Zhao, *More on QCD Ghost Dark Energy*, *Phys. Rev.* **D 86** (2012) 023511 [arXiv:1201.2494] [INSPIRE].

[96] Y. Gong, R.-G. Cai, Y. Chen and Z.-H. Zhu, *Observational constraint on dynamical evolution of dark energy*, *JCAP* **01** (2010) 019 [arXiv:0909.0596] [INSPIRE].

[97] A.C.C. Guimaraes, J.V. Cunha and J.A.S. Lima, *Bayesian Analysis and Constraints on Kinematic Models from Union SNIa*, *JCAP* **10** (2009) 010 [arXiv:0904.3550] [INSPIRE].

[98] M. Szydlowski and W. Godlowski, *Which cosmological models - with dark energy or modified frw dynamics?*, *Phys. Lett.* **B 633** (2006) 427 [astro-ph/0509415] [INSPIRE].

[99] L. Xu, *Unified Dark Fluid with Constant Adiabatic Sound Speed: Including Entropic Perturbations*, *Phys. Rev.* **D 87** (2013) 043503 [arXiv:1210.7413] [INSPIRE].

[100] L. Xu, *Constraints on the holographic dark energy model from type-IA supernovae, WMAP7, baryon acoustic oscillation and redshift-space distortion*, *Phys. Rev.* **D 87** (2013) 043525 [arXiv:1302.2291] [INSPIRE].

[101] R. Gannouji and D. Polarski, *The growth of matter perturbations in some scalar-tensor DE models*, *JCAP* **05** (2008) 018 [arXiv:0802.4196] [INSPIRE].

[102] R.-G. Cai, Q. Su and H.-B. Zhang, *Probing the dynamical behavior of dark energy*, *JCAP* **04** (2010) 012 [arXiv:1001.2207] [INSPIRE].

[103] U. Alam and V. Sahni, *Confronting braneworld cosmology with supernova data and baryon oscillations*, *Phys. Rev.* **D 73** (2006) 084024 [astro-ph/0511473] [INSPIRE].

[104] R. Lazkoz and E. Majerotto, *Cosmological constraints combining H(z), CMB shift and SNIa observational data*, *JCAP* **07** (2007) 015 [arXiv:0704.2606] [INSPIRE].

[105] R.-G. Cai and Q. Su, *On the Dark Sector Interactions*, *Phys. Rev.* **D 81** (2010) 103514 [arXiv:0912.1943] [INSPIRE].

[106] J. Lu, L. Xu and M. Liu, *Constraints on kinematic models from the latest observational data*, *Phys. Lett.* **B 699** (2011) 246 [arXiv:1105.1871] [INSPIRE].

[107] M. Moresco, L. Verde, L. Pozzetti, R. Jimenez and A. Cimatti, *New constraints on cosmological parameters and neutrino properties using the expansion rate of the Universe to* $z \sim 1.75$, *JCAP* **07** (2012) 053 [arXiv:1201.6658] [INSPIRE].

[108] L.P. Chimento, R. Lazkoz and I. Sendra, *DBI models for the unification of dark matter and dark energy*, *Gen. Rel. Grav.* **42** (2010) 1189 [arXiv:0904.1114] [INSPIRE].

[109] L. Chimento and M.I. Forte, *Unified model of baryonic matter and dark components*, *Phys. Lett.* **B 666** (2008) 205 [arXiv:0706.4142] [INSPIRE].

[110] L.P. Chimento and M.G. Richarte, *Dark matter, dark energy and dark radiation coupled with a transversal interaction*, *Phys. Rev.* **D 86** (2012) 103501 [arXiv:1210.5505] [INSPIRE].

[111] L.P. Chimento and M.G. Richarte, *Dark radiation and dark matter coupled to holographic Ricci dark energy*, *Eur. Phys. J.* **C 73** (2013) 2352 [arXiv:1303.3356] [INSPIRE].

JHEP02(2015)071